Supplement to: *"Four North American glaciers advanced past their modern positions thousands of years apart in the Holocene"*

Field photos and historical imagery

Figure S1. Juneau Ice Field Glacier field photos. **A, B.** Collection of sample JIF-01. **C.** Aerial view from helicopter. Approximate location of bedrock transect denoted with dashed line. **D.** Collection of sample JIF-08. Note glacially abraded bedrock and proximity to glacier. All photos from 2020 field work.

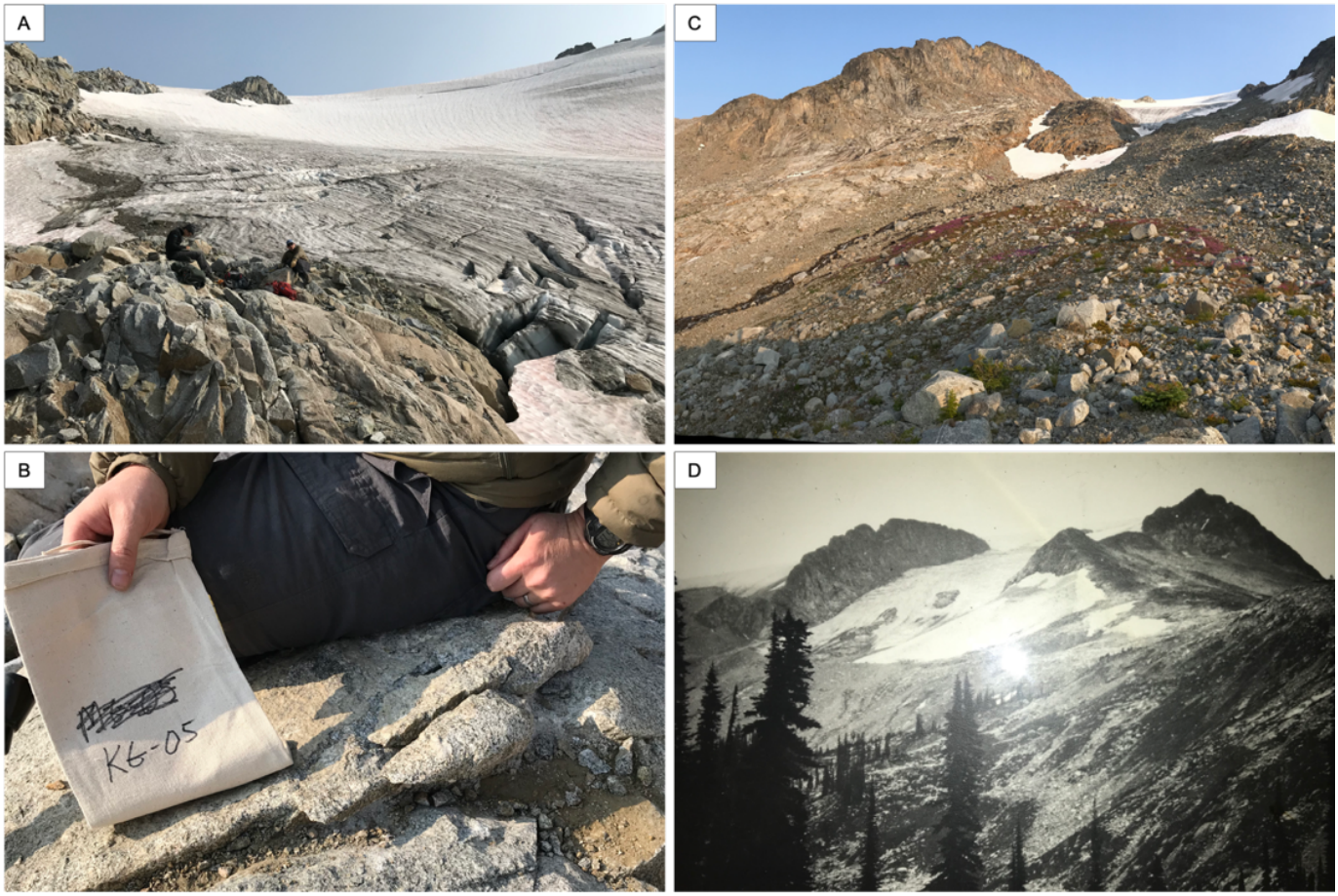

Figure S2. Kokanee Glacier field photos and historical photography. **A.** Collection of sample KG-06. Note abraded bedrock and proximity to glacier. **B**. Collection of sample KG-05. **C.** Glacial forefield. **D.** Historical photo from the Ross Fleming collection, taken between 1922-1926. Field photos (A, B, and C) taken during field work in 2018.

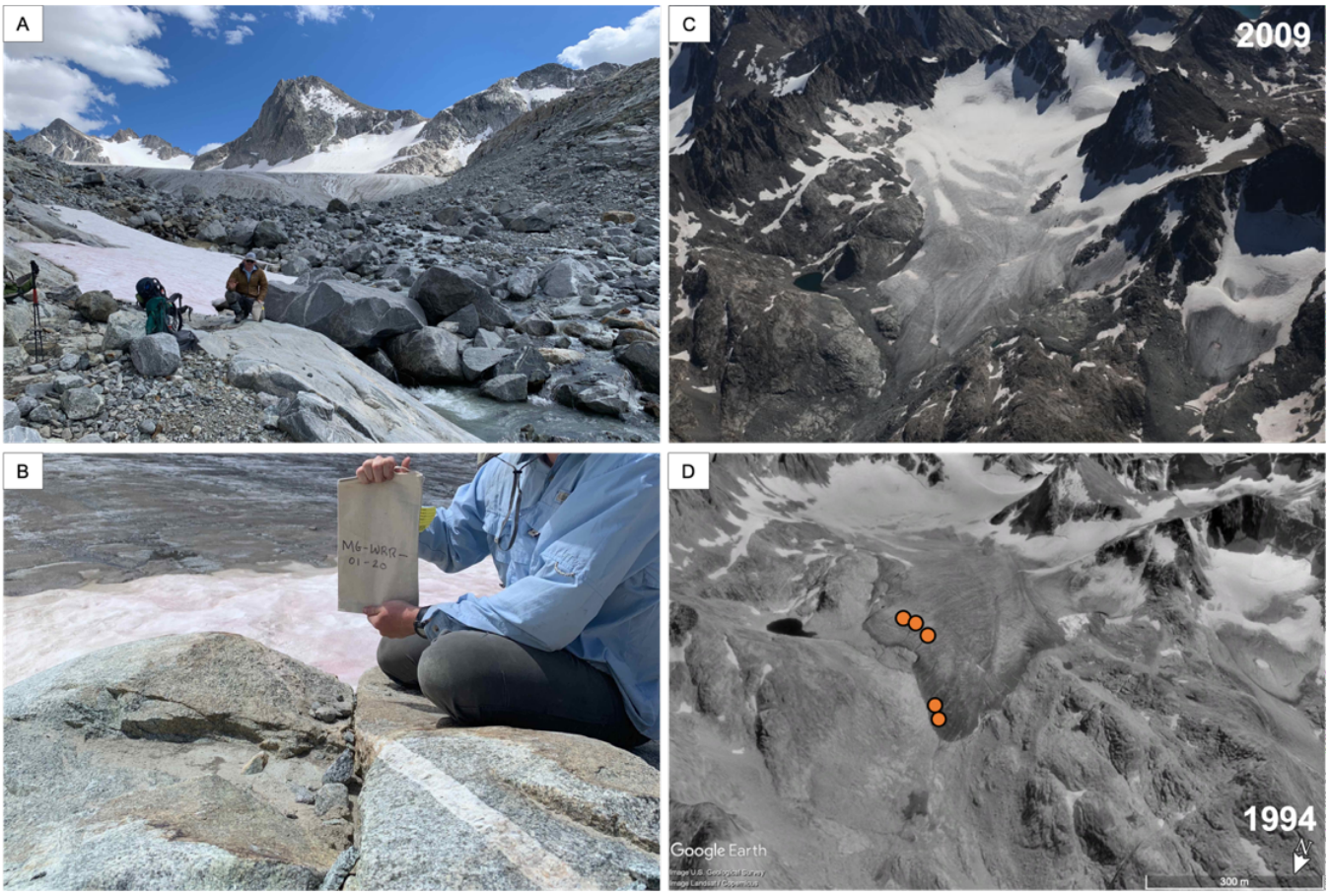

Figure S3. Mammoth Glacier field photos and historical photography. **A.** Collection of sample MG-05. This sample was furthest from the modern glacier of all samples in this study. **B.** Collection of MG-01. Note abraded bedrock and proximity to glacier. **C.** Aerial photography, 2009. Photo Credit: USGS. **D.** Oblique satellite image from 1994 showing all five samples buried under ice (Photo credit: Google Earth and USGS). Field photos (A, B) from field work in 2020.

Figure S4. Conness Glacier field photos and repeat photography. **A, B.** Collection of sample CG-01. Photos from field work in 2018. Note abraded bedrock and proximity to glacier. **C, D.** Repeat photography from the Glacier RePhoto Project (2021). Note the large area loss between 1957 and 2013. Our bedrock sample locations were completely covered in 1957.

Full Monte Carlo forward model results, erosion rate histograms, and other modeling experiments.

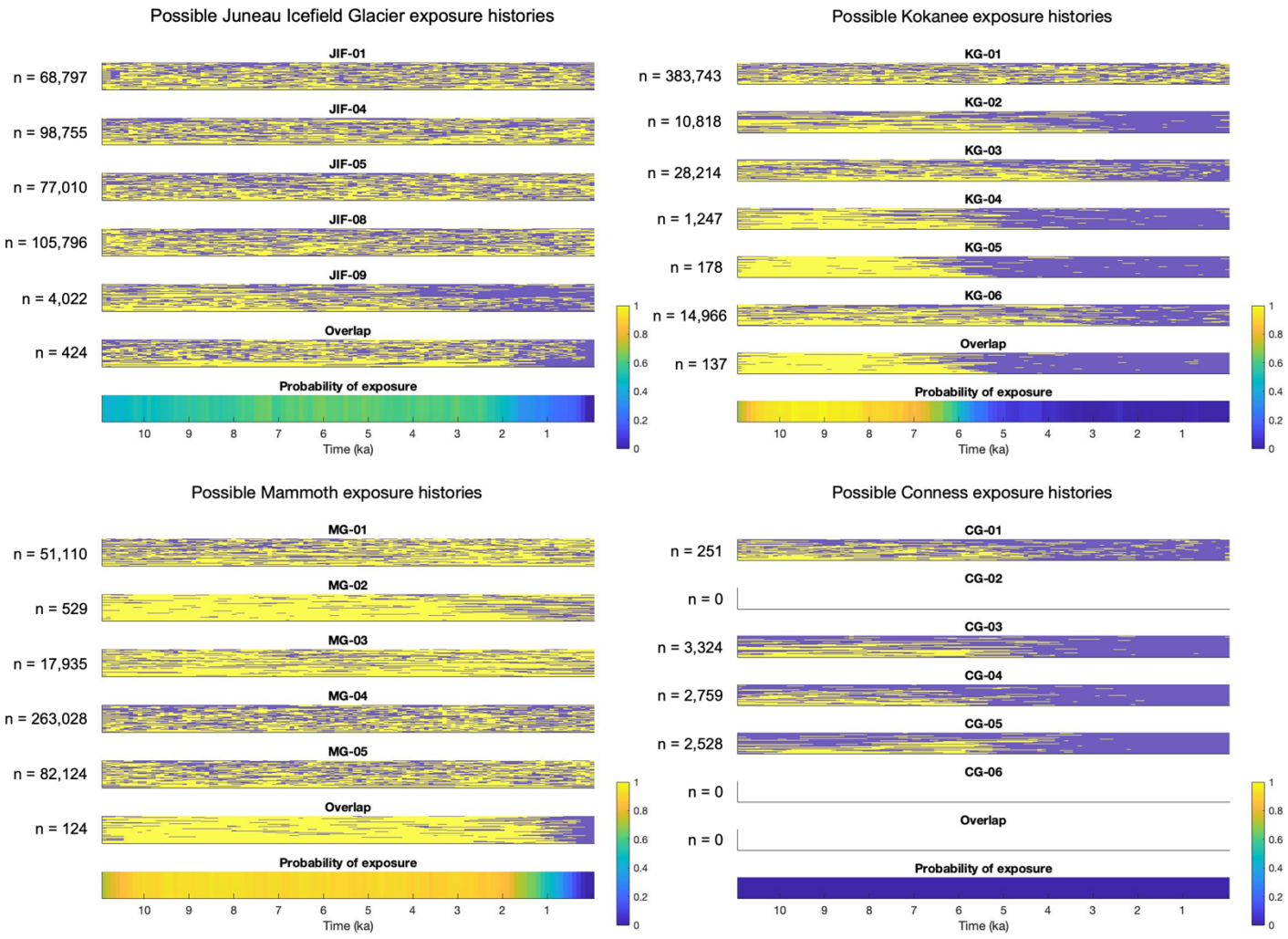

Figure S5. Full Monte Carlo forward model results of possible exposure-burial histories from each sample at each glacier. The plausible exposure-burial scenarios are plotted as horizontal sequences of yellow and blue timesteps, where yellow represents exposure and blue represents burial (see Figure S5 for illustration). For example, sample KG-04 has 1,247 plausible exposure-burial histories; the scenarios depicted mostly show exposure in the early Holocene and burial in the late Holocene with some variation amongst individual scenarios. An exposure-burial scenario can be successful at multiple erosion rates; thus some n-values are > 100,000. The final 'Probability of exposure' is an average of the overlapping scenarios, shown as 'Overlap.' Only scenarios with burial in the final two centuries are included in the overlapping scenarios given geologic evidence for burial prior to sampling."

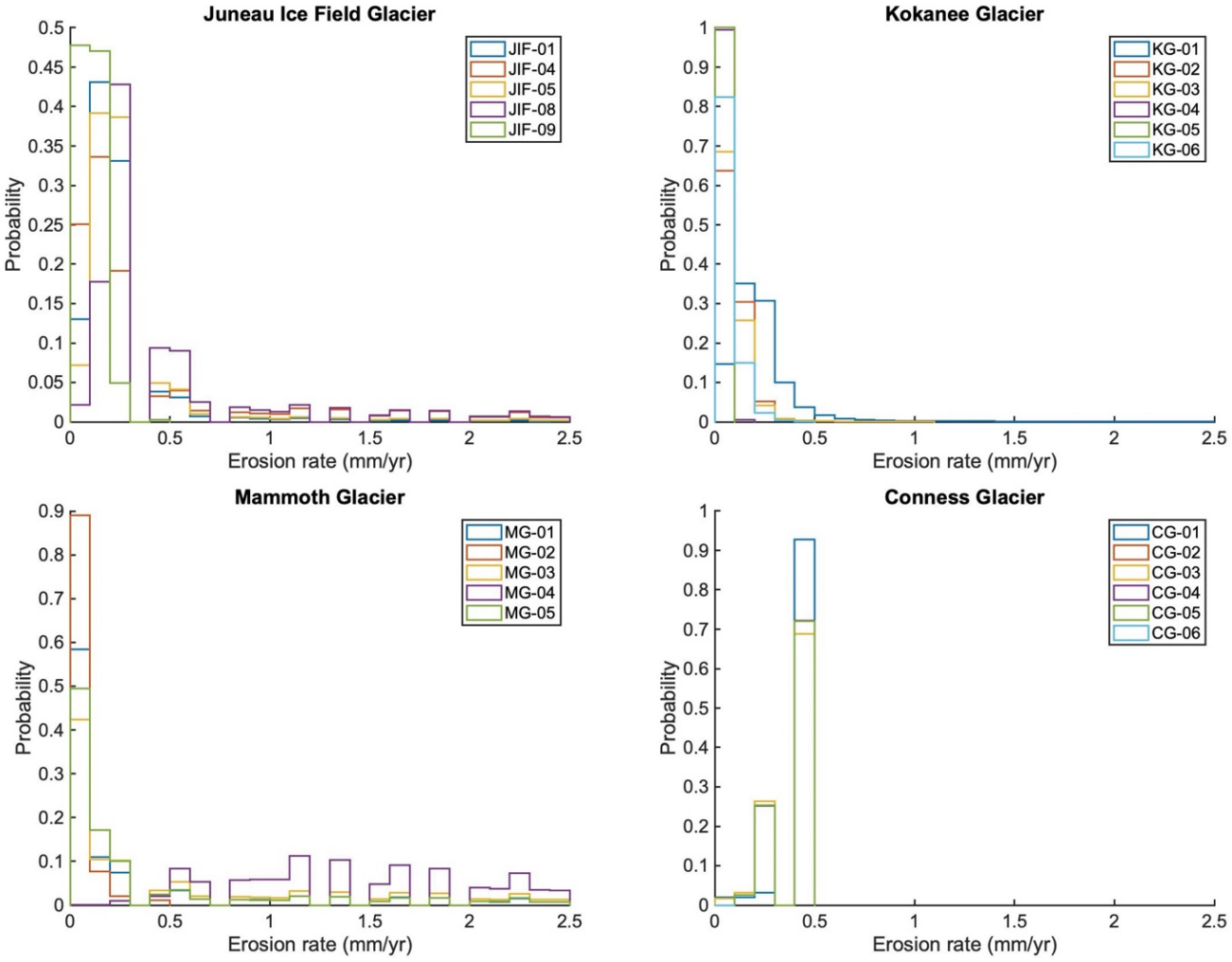

Figure S6. Histograms of erosion rates at each sample capable of recreating measured nuclide concentrations from Monte Carlo forward model simulations. The histograms show *all* the erosion rates at each sample that recreated the measured concentrations, regardless of whether the scenario was saved as an overlapping scenario. The Conness Glacier histogram only includes solutions when erosion rates were capped at 0.5 mm yr^{-1}. A comparison between tests from 0.0–0.5 mm yr^{-1} to tests from 0.0–2.5 mm yr^{-1} are shown in Figure S8.

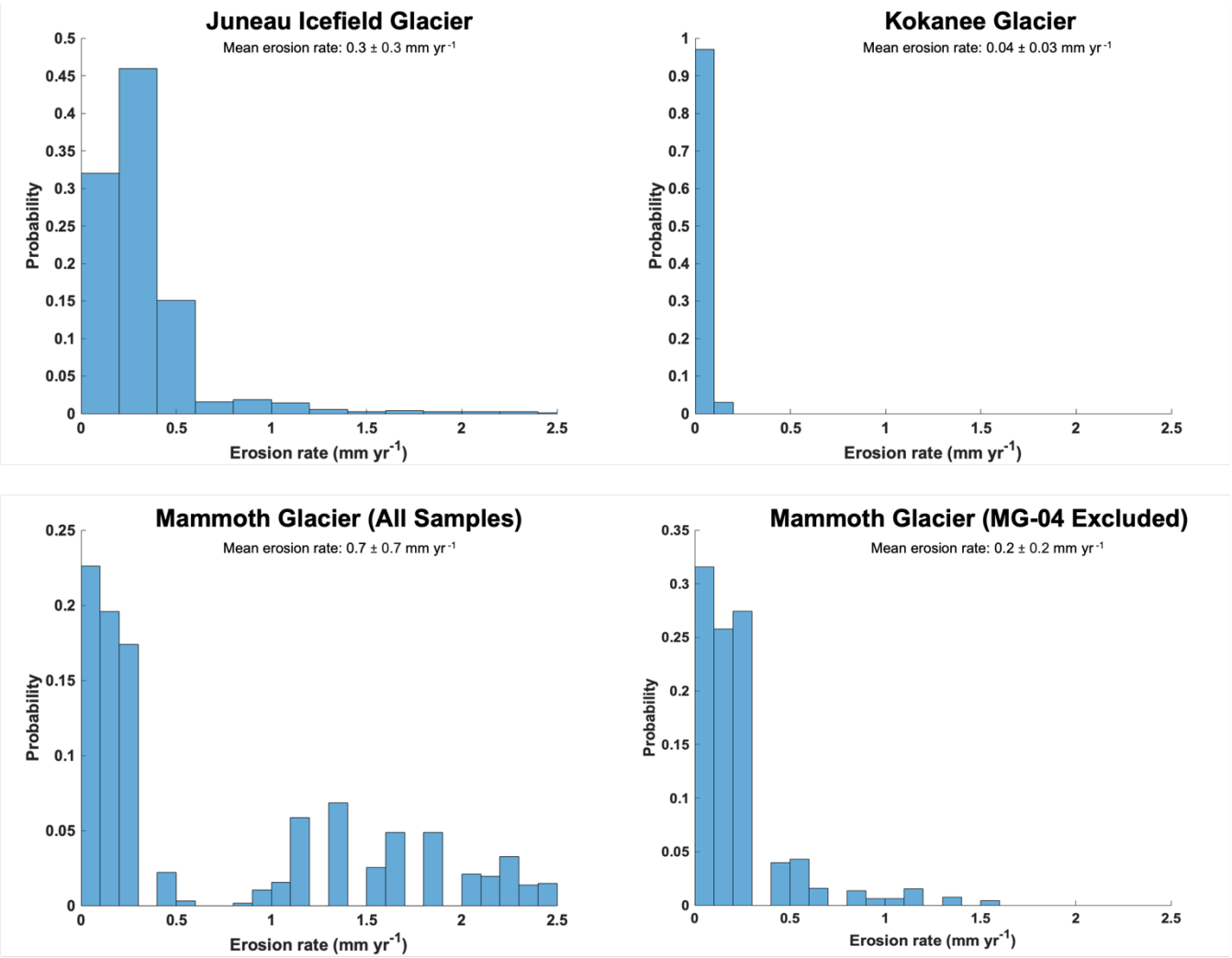

Figure S7. Histograms of erosion rates used in overlapping scenarios for all samples at JIF, Kokanee, and Mammoth Glacier. The data in this plot are used to make the mean erosion rate calculations for each glacier. This figure differs from Figure S6 in that Figure S6 shows the erosion rates capable of recreating measured concentrations at each sample regardless of whether the scenario is overlapping. Here, we show only erosion rates used in the overlapping scenarios (successful scenarios for all samples). The two histograms at Mammoth Glacier compare results when including or excluding sample MG-04. This sample has lower nuclide concentrations that suggest deeper erosion than the other samples, perhaps by subglacial quarrying. As a result, the histogram with MG-04 excluded is interpreted to approximate an abrasion rate in the main text.

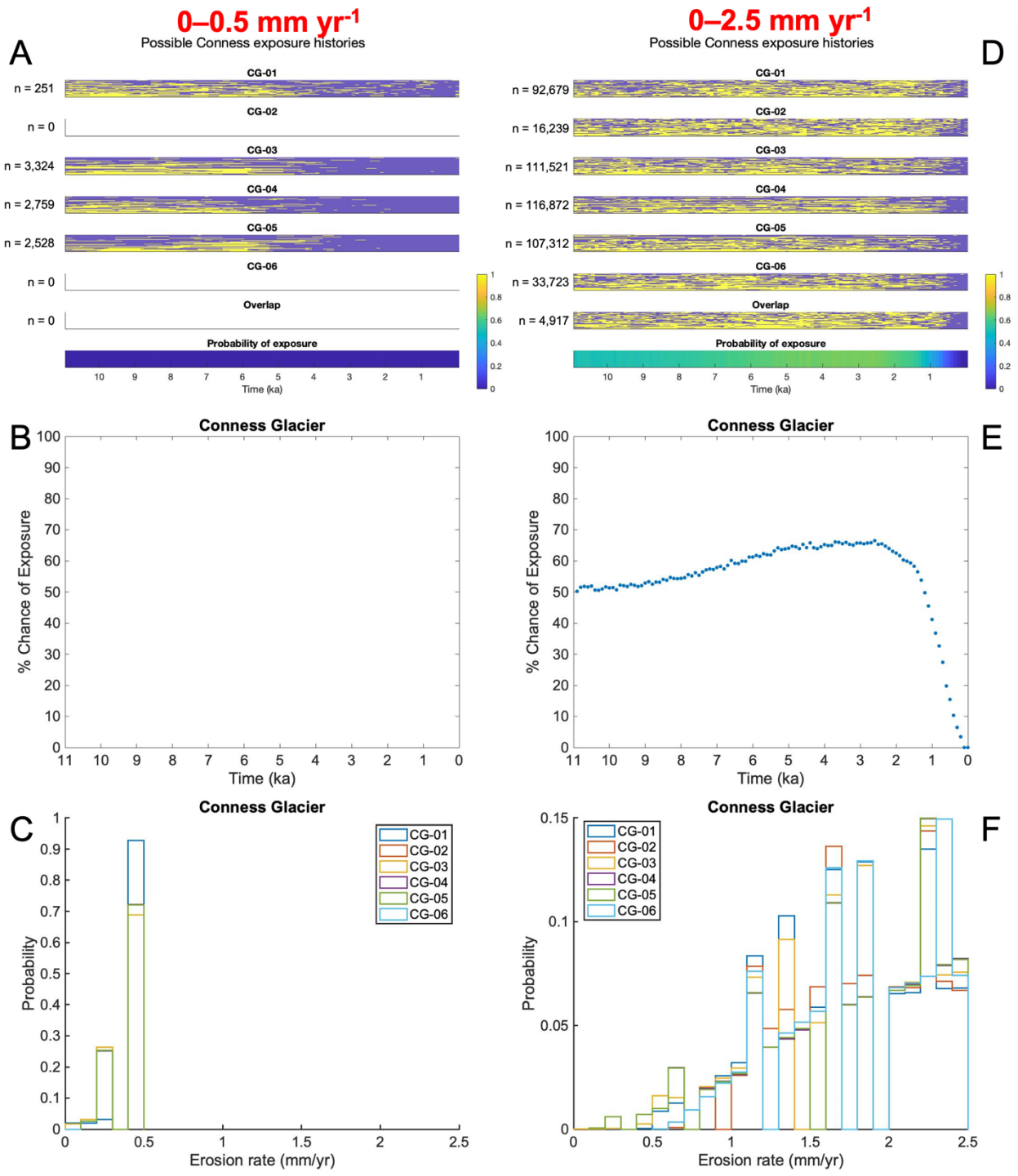

Figure S8. Experiment with limiting erosion rates at Conness Glacier in the Monte Carlo forward model. limiting erosion to 0.5 mm yr^{-1} (left panels, A–C) versus the full range of erosion rates (0 to 2.5 mm yr^{-1}, right panels, D–F). Top panels show all successful exposure-burial histories at each sample and overlapping scenarios. Middle panels show the probability of exposure through time. Bottom panels show histograms of erosion rates used at each sample for the plausible scenarios. See Figures S5 and S6 for further details on the panels. In Panel F, note that the data skews towards higher erosion rates.

Supplemental Tables

Table S1. ^{14}C and ^{10}Be sample data. All uncertainties are 1σ.

Sample	Latitude (DD)	Longitude (DD)	Elevation (m asl)	Thickness (cm)	Shielding
Juneau Ice Field Glacier					
JIF-01	59.48509	-134.91780	1160	3.1	0.9846
JIF-02	59.48210	-134.91800	1160	8.2	0.9836
JIF-03	59.48612	-134.91802	1172	2.9	0.9813
JIF-04	59.48354	-134.91882	1132	2.6	0.9885
JIF-05	59.48354	-134.91882	1132	7.2	0.9905
JIF-06	59.48365	-134.91692	1138	3.6	0.9801
JIF-07	59.48388	-134.91715	1140	2.7	0.9738
JIF-08	59.48434	-134.91700	1149	3.3	0.9817
JIF-09	59.48430	-134.91663	1151	5.4	0.9830
Kokanee Glacier					
KG-01	49.75904	-117.16742	2462	2.5	0.9368
KG-02	49.75897	-117.16751	2476	3.5	0.9368
KG-03	49.75959	-117.16631	2469	2.0	0.9432
KG-04	49.75830	-117.16510	2538	3.0	0.9588
KG-05	49.75846	-117.16521	2536	2.5	0.9545
KG-06	49.75893	-117.16585	2502	2.0	0.9554
Mammoth Glacier					
MG-01	43.17538	-109.66965	3516	2.8	0.9794
MG-02	43.17537	-109.67020	3509	2.5	0.9791
MG-03	43.17583	-109.67105	3496	2.0	0.9781
MG-04	43.17838	-109.67337	3433	2.0	0.9785
MG-05	43.17883	-109.67379	3435	2.5	0.9785
Conness Glacier					
CG-01	37.96794	-119.31320	3547	1.5	0.9527
CG-02	37.96840	-119.31396	3536	2.5	0.9624
CG-03	37.96825	-119.31511	3555	1.0	0.9331
CG-04	37.96868	-119.31751	3536	2.0	0.9154
CG-05	37.96878	-119.31840	3529	3.0	0.9317
CG-06	37.96866	-119.31855	3537	2.0	0.9206

Table S2. ^{10}Be laboratory measurement details. All uncertainties are 1σ.

Sample	Quartz Mass (g)	Be Added (g)	^{10}Be/^{9}Be[a] (10^{-13})	Uncertainty (10^{-15})	^{10}Be Blank
Juneau Ice Field Glacier					
JIF-001	30.1262	0.2534	0.719	4.980	BLK_092320
JIF-002	6.5279	0.2524	0.142	2.100	BLK_092320
JIF-003	12.4480	0.2515	0.038	0.990	BLK_092320
JIF-004	30.1750	0.2512	0.883	4.420	BLK_092320
JIF-005	30.2996	0.2505	0.682	3.970	BLK_092320
JIF-006	30.6159	0.2499	0.070	1.250	BLK_092320
JIF-007	30.2047	0.2481	0.216	2.210	BLK_092320
JIF-008	30.2035	0.2500	0.545	4.370	BLK_092320
JIF-009	30.4616	0.2501	0.746	4.510	BLK_092320
Kokanee Glacier					
KG-01	20.0064	0.1946	1.260	4.410	29_1, 29_2
KG-02	20.0836	0.1952	1.160	4.210	29_1, 29_2
KG-03	17.2460	0.1949	1.410	4.550	29_1, 29_2
KG-04	20.0766	0.1949	2.120	5.760	29_1, 29_2
KG-05	20.0070	0.1945	2.660	6.690	29_1, 29_2
KG-06	20.0311	0.1944	1.900	5.100	29_1, 29_2
Mammoth Glacier					
MG-01	34.8843	0.1918	9.120	26.300	31_1, 31_2
MG-02	38.0706	0.1928	14.900	42.300	31_1, 31_2
MG-03	34.6902	0.1930	11.400	26.300	31_1, 31_2
MG-04	24.4404	0.1924	0.620	4.290	31_1, 31_2
MG-05	34.7489	0.1923	6.830	17.600	31_1, 31_2
Conness Glacier					
CG-01	20.0062	0.1944	0.109	1.130	29_1, 29_2
CG-02	20.0034	0.1937	0.093	1.080	29_1, 29_2
CG-03	14.6740	0.1950	0.055	0.765	29_1, 29_2
CG-04	20.0049	0.1945	0.036	0.748	29_1, 29_2
CG-05	20.0256	0.1951	0.039	0.712	29_1, 29_2
CG-06	20.0180	0.1936	0.043	0.674	29_1, 29_2

[a]Measured relative to standard 07KNSTD with an assumed ^{10}Be/^{9}Be ratio of 2.85 x 10^{-12} (Nishiizumi et al., 2007).

Table S3. ^{10}Be Blank Data. All uncertainties are 1σ.

Blank ID	Be Added (g)	^{10}Be/^{9}Be[a]	Uncertainty	^{10}Be (10^4 atoms)	Uncertainty (10^4 atoms)
Blank_29_1	0.7648	9.86E-16	4.00E-16	1.270	0.515
Blank_29_2	0.7698	1.29E-15	3.58E-16	1.670	0.463
Blank_32_1	0.7618	7.52E-16	7.20E-16	0.963	0.922
Blank_32_7	0.7670	1.78E-15	7.25E-16	2.290	0.935
BLK_092320[b]	0.2770	1.51E-15	6.10E-16	2.530	1.170

[a]Measured relative to standard 07KNSTD with an assumed ^{10}Be/^{9}Be ratio of 2.85 x 10^{-12} (Nishiizumi et al., 2007).

[b]Carrier used is TUBe (904 ppm ^{9}Be). All other blanks used OSUWhite (251.6 ppm ^{9}Be)

Table S4. ^{14}C laboratory measurement details. All uncertainties are 1σ.

Sample	Quartz Mass (g)	C Yield (µg)	Diluted C (µg)	$^{14}C/C$	Uncert.	^{14}C (10^4 atoms/g)	Uncert. (10^4 atoms)	Effective Blank (10^4 atoms)	Uncert. (10^4 atoms)
Juneau Ice Field Glacier									
JIF-01	5.0218	26.9	113.2	7.52E-14	4.64E-16	7.53	0.142	4.77	0.374
JIF-02	3.5704	46.6	115.3	9.45E-14	7.79E-16	13.90	0.254	4.77	0.374
JIF-03	3.6063	120.3	120.3	4.52E-14	4.54E-16	6.16	0.160	4.77	0.374
JIF-04	5.0276	19.3	111.2	1.01E-13	7.80E-16	10.20	0.183	4.77	0.374
JIF-05	4.9143	14.0	113.3	7.21E-14	4.95E-16	7.35	0.143	4.77	0.374
JIF-06	4.9524	11.1	113.6	3.05E-14	4.42E-16	2.53	0.102	4.77	0.374
JIF-07	4.9232	17.5	113.5	4.08E-14	3.82E-16	3.74	0.107	4.77	0.374
JIF-08	4.9016	21.7	114.7	6.09E-14	4.97E-16	6.15	0.132	4.77	0.374
JIF-09	4.9644	7.9	113.7	5.77E-14	5.23E-16	5.66	0.128	4.77	0.374
Kokanee Glacier									
KG-01	4.7200	7.0	111.4	1.01E-13	6.22E-16	10.90	0.187	4.77	0.374
KG-02	5.0853	4.8	97.5	8.19E-14	5.14E-16	6.89	0.134	4.77	0.374
KG-03	2.8927	3.7	94.2	7.28E-14	5.39E-16	10.20	0.218	4.77	0.374
KG-04	5.0205	4.1	113.2	1.00E-13	6.52E-16	10.30	0.178	4.77	0.374
KG-05	4.0061	3.0	111.1	9.33E-14	5.38E-16	11.70	0.204	4.77	0.374
KG-06	4.1491	4.3	112.7	9.35E-14	5.46E-16	11.50	0.200	4.77	0.374
Mammoth Glacier									
MG-01	4.9461	41.0	114.9	5.00E-13	1.76E-15	56.80	0.771	4.77	0.374
MG-02	5.0272	37.3	113.5	5.37E-13	1.93E-15	59.70	0.810	4.77	0.374
MG-03	5.0664	28.0	111.6	6.01E-13	2.10E-15	65.30	0.883	4.77	0.374
MG-04	4.9380	32.3	112.3	8.40E-14	8.96E-16	8.68	0.178	4.77	0.374
MG-05	5.1169	38.9	112.7	4.40E-13	1.60E-15	47.60	0.650	4.77	0.374
Conness Glacier									
CG-01	4.9625	4.9	113.6	2.60E-14	3.12E-16	2.65	0.109	1.57	0.474
CG-02	3.9543	3.5	112.7	2.32E-14	5.39E-16	2.91	0.149	1.57	0.474
CG-03	3.6099	2.8	103.5	2.24E-14	3.73E-16	1.59	1.010	5.85	3.640
CG-04	5.1309	3.1	100.4	1.55E-14	2.41E-16	0.37	0.709	5.85	3.640
CG-05	5.0159	3.3	101.6	2.27E-14	2.89E-16	1.13	0.726	5.85	3.640
CG-06	3.9691	3.6	112.9	2.07E-14	3.91E-16	2.55	0.137	1.57	0.474

Table S5. Glacier area calculations and details.

Glacier	Year	Area[a] (km^2)	Change from LIA Area (%)	Citation	Image Source
JIF Glacier	2021	14.05	76.9	This study	Copernicus
	2003	14.77	80.9	This study	Copernicus
	1880	18.26	100.0	This study	Copernicus
Kokanee Glacier	2021	2.63	39.1	This study	Copernicus
	2008	2.77	41.2	This study	Copernicus
	1880	6.73	100.0	This study	Copernicus
Mammoth Glacier	2014	1.67	49.0	DeVisser and Fountain, 2015	Maps, aerial photos
	2006	2.00	58.7	DeVisser and Fountain, 2015	Maps, aerial photos
	2001	2.06	60.4	DeVisser and Fountain, 2015	Maps, aerial photos
	1994	2.29	67.2	DeVisser and Fountain, 2015	Maps, aerial photos
	1966	2.54	74.5	DeVisser and Fountain, 2015	Maps, aerial photos
	1950	2.88	84.5	DeVisser and Fountain, 2015	Maps, aerial photos
	1880	3.41	100.0	DeVisser and Fountain, 2015	Maps, aerial photos
Conness Glacier	2021	0.11	16.8	This study	Copernicus
	2004	0.16	24.6	Basgaic and Fountain, 2011	Basagic Survey
	1972	0.1977	30.4	Basgaic and Fountain, 2011	Historical Photo
	1954	0.2304	35.4	Basgaic and Fountain, 2011	Historical Photo
	1944	0.2611	40.2	Basgaic and Fountain, 2011	Historical Photo
	1880	0.65	100.0	This Study	Copernicus
Wind River Composite	2006	20.40	55.6	DeVisser and Fountain, 2015	NA
	2001	21.29	58.1	DeVisser and Fountain, 2015	NA
	1994	23.37	63.7	DeVisser and Fountain, 2015	NA
	1966	27.32	74.5	DeVisser and Fountain, 2015	NA
	1880	36.67	100.0	DeVisser and Fountain, 2015	NA
Sierra Nevada Synthetic	2004	31.32	44.0	Basgaic and Fountain, 2011	NA
	1972	39.15	55.0	Basgaic and Fountain, 2011	NA
	1880	71.18	100.0	Basgaic and Fountain, 2011	NA